



## Foot Arch Classification via ML-based Image Classification

Wudhichart Sawangphol<sup>1</sup> , Pilailuck Panphattarasap<sup>2</sup> , Pisit Praiwattana<sup>3</sup> , Jidapa Kraisangka<sup>4</sup> ,  
Thanapon Noraset<sup>5</sup> , Danu Prommin<sup>6</sup> 

<sup>1</sup>Faculty of Information and Communication Technology, Mahidol University, [wudhichart.saw@mahidol.ac.th](mailto:wudhichart.saw@mahidol.ac.th)

<sup>2</sup>Faculty of Information and Communication Technology, Mahidol University, [pilailuck.pan@mahidol.ac.th](mailto:pilailuck.pan@mahidol.ac.th)

<sup>3</sup>Faculty of Information and Communication Technology, Mahidol University, [pisit.pra@mahidol.ac.th](mailto:pisit.pra@mahidol.ac.th)

<sup>4</sup>Faculty of Information and Communication Technology, Mahidol University, [jidapa.kra@mahidol.ac.th](mailto:jidapa.kra@mahidol.ac.th)

<sup>5</sup>Faculty of Information and Communication Technology, Mahidol University, [thanapon.nor@mahidol.ac.th](mailto:thanapon.nor@mahidol.ac.th)

<sup>6</sup>National Metal and Materials Technology Center, National Science and Technology Development Agency, [danup@mtec.or.th](mailto:danup@mtec.or.th)

Corresponding author: Pisit Praiwattana, [pisit.pra@mahidol.ac.th](mailto:pisit.pra@mahidol.ac.th)

**Abstract.** Foot pain have become one of the common health problem. One of the commonly-used noninvasive method to relieve foot pain is to insert insoles in ones' shoes. However, choosing the right insoles strongly depends on foot arch types, i.e., high arch, normal arch, and flat foot. Aside from manual classification, using foot images become an alternative methods to classify the foot type. We propose to develop mathematical models using machine learning techniques to improve the accuracy and reduce the time of the foot arch classification from foot pressure scanning image. 200 foot images were used to develop the models by applying decision tree, random forest, support vector machine, artificial neural network, and XGBoost algorithm. We found that the decision tree classifier with the features including different areas of part of feet, arch index, whole foot area, and side of foot has the best performance than the other classifiers in terms of accuracy, precision, recall, F1 score, and the number of features. The results also demonstrates that the obtained model can classify foot arch types with high accuracy at 95% on the testing experiment.

**Keywords:** Foot arch, Foot arch type, Image classification, Foot pressure scanning image

**DOI:** <https://doi.org/10.14733/cadaps.2023.600-613>

## 1 INTRODUCTION

Feet are one of essential organs, which help humans to maintain and relocate the center of their body. Every day, people rely on their feet to support a weight and movement of their body. In 2011, several research stated that the percentage of working people and elderly people, who have foot health problems (such as foot

pain) has continuously increased, i.e., 24% or one quarter of number of people [24]. *Foot pain* causes many problems, which have a great impact on working and daily life, including sports and other activities [5, 9]. Furthermore, in elderly people, foot pain and foot health problems may increase the risk of falling and other health problems.

There are many causes of foot pain, such as physical activities or abnormal bone structure and muscle. Foot posture [18] is considered to be an important component of musculoskeletal assessment in clinical practices and research. The foot helps a person maintain and shift one's center of gravity. When the structure or the state of the human body changes, plantar pressure distribution changes accordingly. Foot posture alignment is related to foot deformity problems in that the foot lades the weight and contains the stability.

In order to noninvasively aid patients suffering from foot pain, a *foot orthosis*, such as an *insole*, is placed under patients' feet to support their feet and body. The insole with a proper shape and size customized to a person, i.e., a *personalized insole*, can relieve foot pain [22, 13, 12]. There are many important factors to be considered for making a *personalized* foot insole. One of them is *foot arch* structure [27] (Fig. 1), classified into 3 types: *normal arch*, *flat arch* and *high arch* [10]. The normal arch will leave a print of one's heel and forefoot connected by a slightly narrower area. The flat arch or low arch is a flexible foot, which is wider and straighter than a footprint with an arch sitting low to the ground. Lastly, the high arch demonstrates a very narrow curved footprint with an arch sitting higher from the ground. The shapes of feet are important for good health. Unfortunately, some people have abnormal shapes of feet, such as "flat arch" and "high arch". These badly affect the performance of walking and maintaining posture. People having a high arch may experience an imbalance in their body, causing the sprained ankle after standing for a long time. The flat arch may cause lower back and knee pains. These foot deformity problems can be caused by pedialgia, which is relevant to knee pain, ischialgia, and lumbago.



**Figure 1:** Foot Arch Types.

Therefore, understanding the foot morphology and foot arch is necessary not only for clinical and rehabilitative purpose but also for designing personalized and comfortable insole and footwear. In addition, simple and quantitative classifications of foot arches can help to provide appropriate footwear for each arch structure to avoid harm to foot health [10]. Investigation into the effects of foot structure on foot function has been at the core of many studies, sometimes with conflicting results [10, 14].

The traditional method for analyzing foot arch types is manual measurement and calculation, which strongly relies on *Arch Index* [14], an index representing the area of the middle third of the footprint. The method separates the footprint in a ratio form, excluding the toes. It classifies arch types that relate to foot pressures and rear foot motion from stepping to moving the position. In addition, the arch index also correlates with the height of the navicular and foot angular measures from the radiograph. The arch index is measured by using a graphic tablet or optical scanner to observe the footprint and calculate the footprint area by imaging software. Arch Index can be calculated using the equation  $AI = B/(A + B + C)$  [14], where  $A$ ,  $B$ , and  $C$  are the area of parts of the foot (shown in Fig. 8). The index scores have a range between 0 to 0.39 with mean=0.24, median=0.24, and standard deviation (SD)=0.06. The feet are considered "normal" when the arch index score is ( $\pm 1$  SD from the mean) 0.21 to 0.28, "high" ( $< 1$  SD) when the score is lower than 0.21 and "low" ( $> 1$  SD) when the score is more than 0.28 [14].

In addition, some researchers proposed intelligent recognition with automatic analysis for foot type detection

on X-ray images, especially identifying flat foot [10]. There are measurements related to foot types, such as arch, arch angle, and footprint. From X-ray images, the ends of the lower edge of the fifth metatarsal line and the ends of the lower edge of the calcaneus line can be calculated by the intersection angle of these two lines. If the angle is greater than 165 degrees, it is considered flatfoot. Moreover, the footprint is used for measuring the lengths of the arch empty and the middle of the foot. If those two lengths are similar, the footprint is the normal foot. On the other hand, the flatfoot has different lengths between the length of the arch empty that is less than 1 centimeter when compared with the length of the middle foot. Although the flatfoot identification by the proposed algorithm shows a good performance in most cases, those methods need a lot of foot X-ray images for training and testing to achieve high accuracy on discrimination. It takes a lot of effort to scan more than pressing feet on the foot scanner.

Moreover, there was a development of the visual categorization tool based on the arch index to increase the reliability and validity of foot categorization [14]. The tool measures the arch index using footprint from a *carbon paper imprint material*. There are two main points that need to be considered. The first one is using carbon paper for imprinting, giving an unclear footprint, especially on the middle part of the foot, which foot categorization with the arch index might measure the incorrect foot type. The second point is this research obtained only older participants, and the foot categorization is based on the older arch index standard. Other age's arch index might not use this foot categorization because each age has a different arch index, which the tool might define the erroneous foot types.

Another research is proposed to automatically calculate the arch index via image processing from foot pressure images from the Press Cam analysis tool [20]. This work also focuses on using foot-pressure images as inputs. However, this research requires knowledge from experts to ensure the correctness of the foot type classification.

These methods require human expertise. Moreover, they are time-consuming and prone to human errors. Thus, personalized insoles are not widely used. Unlike previous work, this work proposes a data-driven method to build foot arch-type classification models from a foot pressure scanning image as shown in Fig. 5a. The proposed method not only improves the accuracy but also reduces the time of the foot arch type classification. In addition, we proposed a system to deploy our mathematical model for foot arch classification.

The remainder of this paper is structured as follows. The proposed Foot Arch Classification Model Development section explains the details of our proposed model development. The Experimental Setup section presents the setup of our experiments, and the Experimental Result section provides in-depth details on the Experimental results, including a discussion. Next, the system called *Foot Arch Type Classification System* (FAC) is presented to show how the foot arch classification model is equipped. Finally, the conclusion and future direction are summarised and presented.

## 2 THE PROPOSED FOOT ARCH CLASSIFICATION MODEL DEVELOPMENT

In this section, we present the process of our proposed *Foot Arch Classification Model development*. The details of each process are introduced in the following subsections. There are two main processes: 1. *Data Collection and Feature Engineering*, and 2. *Model Development and Model Selection*. We used images obtained from the foot pressure scanner as our data source, as shown in Fig. 5a. The images are processed into a one-dimensional vector feature via image processing. Next, the extracted features will be selected for the classification model development. The output of the process of Data Collection and Feature Engineering is the feature set, and it becomes an input of the process of Model Development and Model Selection. The Model Development and Model Selection process performs the foot arch classification model development and selection by utilizing various classification algorithms [21] and the feature sets. From this process, the selected classification model will be an output for the system development.

## 2.1 Data Collection and Feature Engineering

The details of this process are shown in Fig. 2. The details on extracting a feature set from the foot pressure scanning images are provided as follows.

**Data Collection:** We gather foot pressure scanning images from the Presscam analysis tool (Fig. 3c) [26]. Once a volunteer stands on SIDAS Foot Scanner (Fig. 3a and Fig. 3b), the scanner will capture and scan the plantar surface of the feet. Then, the obtained plantar surface of the feet is transferred to the Presscam analysis tool. Finally, the foot pressure scanning images (as shown in Fig. 4) are exported for analysis.

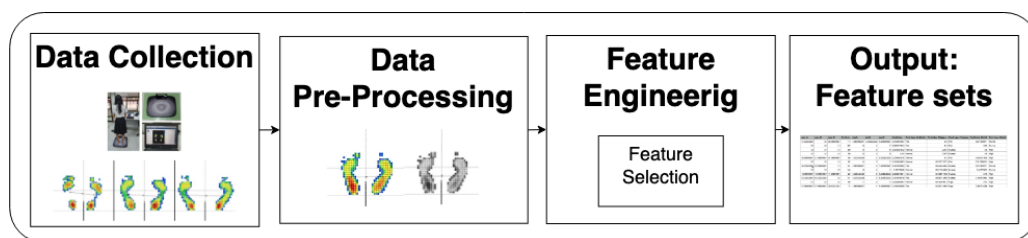


**Figure 2:** Details of Data Collection and Feature Engineering Process.

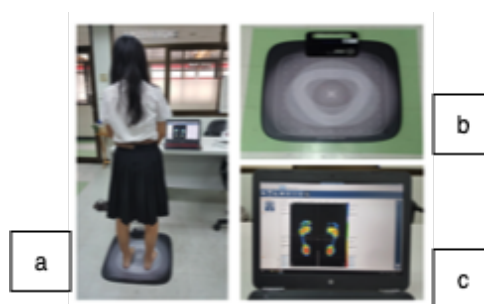


**Figure 3:** (a) How a volunteer stands on the scanner, (b) SIDAS Foot Scanner, and (c) Presscam analysis tool (Source: [20]).

We collect foot pressure scanning images from 100 volunteers with different foot arch types. Each foot pressure scanning image contains 2 feet and each side of the feet is considered a separate image. Therefore, there are 200-foot pressure scanning images in total with 93 of normal arch type (Fig. 4a), 84 of high arch type (Fig. 4b), and 23 of flat arch type (Fig. 4c).

**Data Pre-processing:** We applied the data-preprocessing techniques similar to the one presented in [20]. The process is divided into two steps as follows:

1) *Map-to-One*. This step converts each square in the foot pressure scanning images in the RGB format to a pair of foot silhouettes. As shown in Fig. 5a, the input foot pressure scanning image has a size of 500x500 pixels, but the pressure sensor has a much lower resolution. The image is converted to grayscale as shown in Fig. 5b. As can be seen in Fig. 5b, in each grayscale image, we map the square blocks into pixels to obtain the final *binary image* consisting of black and white pixels.

The size of a square block is 13x13 pixels. If the block contains a part of the foot, a square block is converted into a 1x1 pixel with a black color. Otherwise, the block is converted into a 1x1 pixel with white colour. The average color value of each square block is also calculated. For the case of overlapping pixels, the color values will be used in the calculation of the average color value for those square blocks. We set

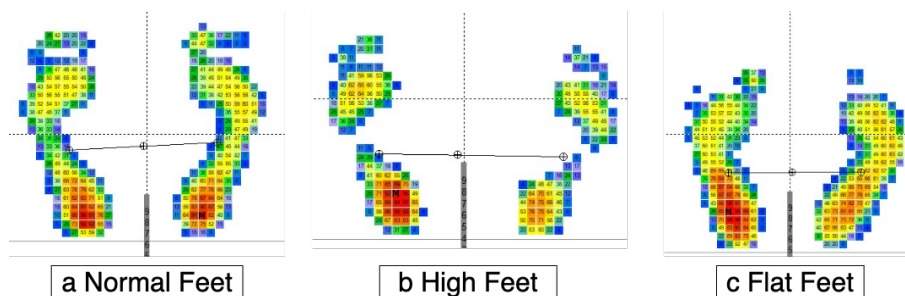


**Figure 4:** Examples of Foot Pressure Scanning Images in different arch types: (a) Normal feet, (b) High feet, and (c) Flat feet.

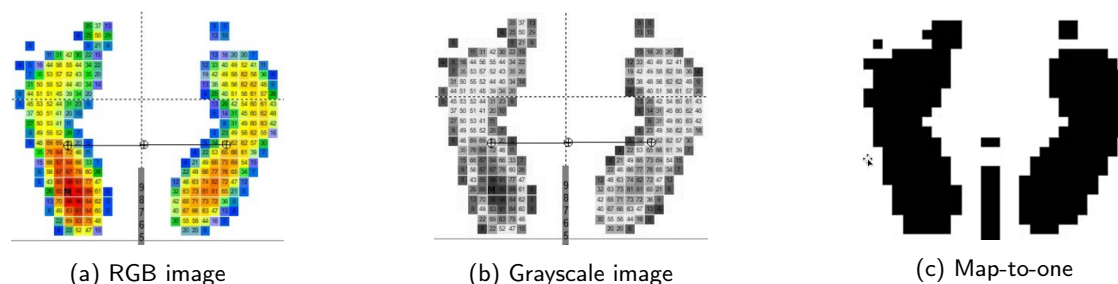


**Figure 5:** An example of data pre-processing (Source: [20]).

the threshold to differentiate the average color value between black and white, i.e., the value of 0.9 is the best threshold to determine whether a square block is part of the foot. Thus, if the average color value of a square block is less than 0.9, a square block is converted into 1x1 pixel with the color value of 0 (Note that 0 represents the black color or part of the foot and 1 represents the white color or non-part of the foot). Otherwise, it is converted into a 1x1 pixel with a color value of 1. As a result, we obtain the 40x40 pixel binary image as shown in Fig. 5c.

2) *Removing Toes*. This process detects the toes of foot binary image and removes them. We apply the process described in this research [20] by removing any components in the upper one-fourth of the foot area that has a width less than half of the foot width. The output of this step is the feet binary image without toes, as shown in Fig. 6.

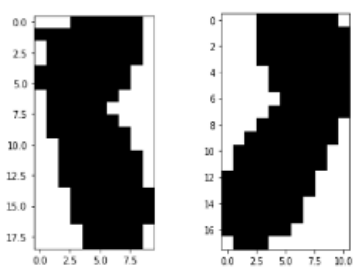


**Figure 6:** An output image from Removing Toes step (Source: [20]).

**Feature Engineering:** In machine learning methodologies, the feature engineering process is essential

for developing machine learning algorithms. It refers to the process that selecting and deriving useful and meaningful features from a given dataset. For this process, we start from the *feature extraction*, which extracts all features from the binary image.

There are 11 features that are extracted from this process as follows: 1. The Maximum Width of the Upper Part of Foot ( $\max A$ ) defined by the maximum width of the forefoot as AB line in Fig. 7, 2. The Maximum Width of the Lower Part of the Foot ( $\max C$ ) determined by the maximum width of the rear foot as EF line in Fig. 7, 3. The Minimum Width of the Middle Part of the Foot ( $\min B$ ) defined by the narrowest width of the midfoot as CD line in Fig. 7, 4. Chippaux-Šmirák index [25] (CSI) as a ratio of features 3 and 1, 5. Staheli Index [17] (SI), as a ratio of features 3 and 2, 6. The area of the forefoot as area A (area\_A) in Fig. 8, 7. The area of midfoot as area B (area\_B) in Fig. 8, 8. The area of rearfoot as area C (area\_C) in Fig. 8, 9. Arch Index [14, 19] (AI), 10. The area of the entire foot (foot\_area), and 11. The foot side (foot\_side). Lastly, the target class is foot arch type (foot\_type), which is flat, normal, and high.

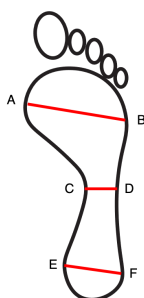


**Figure 7:** Foot Features: a line of AB, CD, and EF.

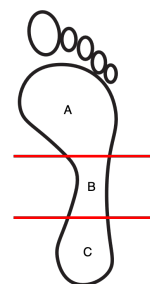


**Figure 8:** Foot Areas: A, B, and C. The line represents the foot axis as the base for division.

## 2.2 Model Development and Model Selection

The details of this process is illustrated in Fig. 9. The mathematical models are automatically constructed based on a variety of machine learning-supervised classification algorithms using training data.

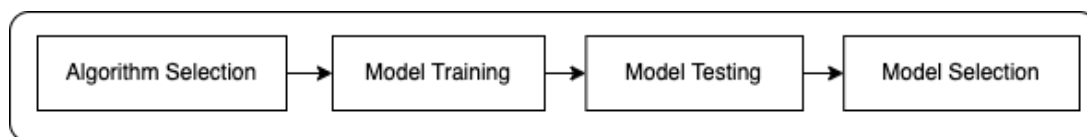


**Figure 9:** Details of Model Development and Model Selection Process.

For *Algorithm Selection* process, we select well-known machine-learning-based classification algorithms as base algorithms for model development as follows: 1. *Decision Tree* (DT) [2], 2. *Random Forest* (RF) [1], 3. *Support Vector Machine* (SVM) [23], 4. *Artificial Neural Network* (ANN) [7], and 5. *XGBoost* [3]. These *supervised classification* techniques identify the information classes of interest in the image [11]. In *Model Training and Model Testing* process, the data set is divided into two groups: a training set and a testing set. Then, the selected algorithms are applied to train models from the training set. We apply cross-validation during the training process. Finally, the trained models are tested by the testing set using four evaluation metrics, including *Classification Accuracy*, *Precision*, *Recall* and *F1 Score* [4]. The details of these metrics will be described in Section 3. Finally, the *Model Selection* process determines the optimal model with high performance to be used in the system.

### 3 EXPERIMENTAL SETUP

In this section, we present the details of the experimental setup including dataset statistics, the description of the evaluation metrics, and the configuration of the selected classifiers and their tuned hyperparameters.

#### 3.1 Dataset Statistics

As mentioned in the data collection section, all data are obtained from the Presscam analysis tool and SIDAS Foot Scanner. There are 200 foot pressure scanning images, which are 93 normal foot images, 84 high foot images, and 23 flat foot images. For each image, 11 features (`maxA`, `maxC`, `minB`, `CSI`, `SI`, `area_A`, `area_B`, `area_C`, `AI`, `foot_area`, and `foot_side`) are extracted. We divide the 200-record data set into a training set and a testing set with a ratio of 80:20 (or 140 images for training and 60 images for testing).

#### 3.2 Configurations

This section further explains how classifiers are trained and integrated into the system, and how the hyperparameters are tuned. In our experiments, the Python packages called Scikit-learn [16] and XGBoost [3] are used. Scikit-learn and XGBoost have classifiers which support all selected classification algorithms.

In machine learning methodology, hyperparameter tuning is essential since it determines the capacity of the model, the capacity to learn, and resource usage. We apply the technique called the grid search [15] to obtain the optimal model configuration and hyperparameter tuning. The grid search examines a subset of data from the training set to find the best metric to measure performance and determine the best hyperparameters. Thus, the model is trained based on the tuned hyperparameters and the data in the training set using 10-fold cross-validation. Subsequently, the final performance will be evaluated using the information from the testing set. The list of tuned hyperparameters using grid search is shown as follows:

1. *DecisionTreeClassifier*: Splitting criterion = gini; Maximum depth of the tree = 5; Minimum sample leaf= 4; Minimum sample split = 3; Maximum features = none
2. *RandomForestClassifier*: Splitting criterion = gini; Number of ensemble trees = 100; Maximum depth of the tree = 5; Minimum sample leaf= 4; Minimum sample split = 3; Maximum features = none
3. *SVC*: Regularization = 100; Kernel = linear
4. *MLPClassifier*: Activation function = tanh; L2 regularization = 0.05; Learning rate = 0.001; Hidden layer size = 100; Solver = adam
5. *XGBClassifier*: Booster = gbtrees; Learning objective = multi:softprob; Learning rate = 0.01; Validation evaluation metric = accuracy; L2 regularization = 0.1; L1 regularization = 0.1

In the model training, 80% of the data are used with different sets of features, including `All_set`, `AI_set`, `CSI_set`, and `SI_set`. The details of features set are shown in Table 1. In addition, the 10-fold cross-validation is applied in this process.

### 4 EXPERIMENTAL RESULTS

In this section, we conduct the experiments to develop classification models and evaluate their performance. Experiments are conducted in two steps. First, we explore the effectiveness of each feature set, namely `All_set`, `AI_set`, `CSI_set`, and `SI_set`, using 10-fold cross-validation on the training set (160 samples). Then, we select the models with high performance to test against a testing set (40 samples). The notion of using different sets of features is to find a small number of features that give high performance.

**Table 1:** Feature sets.

Feature sets	maxA	maxC	minB	CSI	SI	area_A	area_B	area_C	AI	foot_area	foot_side
All_set	✓	✓	✓	✓	✓	✓	✓	✓	✓	✓	✓
AI_set						✓	✓	✓	✓	✓	✓
CSI_set	✓	✓		✓							✓
SI_set		✓	✓		✓						✓

#### 4.1 Cross-validation Results

Table 2 shows the experimental results of the models using All\_set. As can be seen, the decision tree classifier and random forest classifier outperform the other classifiers in terms of accuracy at 97.5%. However, if we compare the other metrics, i.e., recall, precision, and F1 score, it indicates that the random forest classifier is slightly better than the decision tree classifier. The second place is the XGBoost classifier in terms of accuracy at 96.9%, and the other metrics are good as well. Therefore, these three classifiers will be investigated further.

**Table 2:** The cross-validation results.

All_set features					CSI_set features				
Classifier	Accuracy (%)	Recall (%)	Precision (%)	F1 Score	Classifier	Accuracy (%)	Recall (%)	Precision (%)	F1 Score
Decision Tree	97.5	98.4	96.9	0.973	Decision Tree	79.4	75.1	79.7	0.758
SVM	85.4	84.6	80.7	0.81	SVM	79.4	77.2	77.3	0.762
Random Forest	97.5	98.3	98.1	0.981	Random Forest	78.8	73.4	78	0.747
ANN	80.6	81.5	78.2	0.783	ANN	76.9	74.3	74.1	0.733
XGBoost	96.9	98	96.4	0.968	XGBoost	78.1	76.8	76.4	0.753

AI_set features					SI_set features				
Classifier	Accuracy (%)	Recall (%)	Precision (%)	F1 Score	Classifier	Accuracy (%)	Recall (%)	Precision (%)	F1 Score
Decision Tree	97.5	98.4	96.9	0.973	Decision Tree	75.6	71.5	75.6	0.723
SVM	87.5	91	87	0.874	SVM	79.4	78.2	76	0.752
Random Forest	96.9	98	96.4	0.968	Random Forest	78.1	76.7	75.1	0.742
ANN	71.9	66.1	65.2	0.647	ANN	75.6	71.7	72.1	0.705
XGBoost	96.9	98	96.4	0.968	XGBoost	77.5	76.2	77	0.754

From the experiments of AI\_set, although we reduce the number of features from 11 to 6 features, the classification performance is still comparable. In addition, the All\_set and AI\_set outperform CSI\_set and SI\_set for all classifiers. Next, the trained models using the decision tree classifier, random forest classifier, and XGBoost classifier with the All\_set and AI\_set feature sets are tested with the testing set for further analysis.

#### 4.2 Classification Model Testing

As mentioned in the previous section, the trained models using the decision tree classifier, random forest classifier, and XGBoost classifier are tested using the testing set. Note that the experiments were only conducted using the All\_set and AI\_set feature sets. Table 3 demonstrates the testing results of the trained models with the All\_set feature set and the testing results of the trained models with the AI\_set feature set.

**Table 3:** The testing experimental results.

All_set features					AI_set features				
Classifier	Accuracy (%)	Recall (%)	Precision (%)	F1 Score	Classifier	Accuracy (%)	Recall (%)	Precision (%)	F1 Score
Decision Tree	95	96.2	90.1	0.926	Decision Tree	95	96.3	90.2	0.926
Random Forest	95	91.8	96.1	0.935	Random Forest	92.5	88.8	87.8	0.882
XGBoost	95	97.2	89.3	0.926	XGBoost	95	97.2	89.3	0.926

Table 3 shows that overall results for both feature sets are similar. However, in order to obtain the practical model, one factor that is needed to be considered is the number of features that need to be fed to the model. Therefore, it seems that AI\_set outperforms All\_set in terms of the number of features since it requires only half the number of features that are needed for the model with All\_set to obtain a similar performance. Moreover, it indicates that the features in AI\_set is sufficient.

In addition, we then analyze the performance of the decision tree classifier, random forest classifier, and XGBoost classifier. From Table 3, it can be seen that the performances of the decision tree classifier and XGBoost classifier are similar in terms of all evaluation metrics. However, the decision tree classifier has more potential since the result of all evaluation metrics is more than 90% in overall. Moreover, the number of its hyperparameters is also less than that of the XGBoost classifier. Thus, the model trained with the decision tree classifier and AI\_set is selected for the system.

### 4.3 Ablation Analysis

From the previous section, we can model foot arch types by using only features in the AI\_set with the decision tree classifier. To further analyze the contribution of the AI\_set feature, we perform the ablation analysis [6] by discarding features in AI\_set from All\_set. We denote this feature set as AI'\_set. Next, we train models with all classifiers and AI'\_set. The results of cross-validation and testing are shown in Tables 4 and 5, respectively.

**Table 4:** The cross-validation results of AI'\_set.

Classifier	Accuracy (%)	Recall (%)	Precision (%)	F1 Score
Decision Tree	80.6	79.6	81.8	0.792
SVM	81.9	77.8	79.1	0.777
Random Forest	81.9	78.1	80.3	0.783
ANN	78.8	74.1	75.5	0.738
XGBoost	77.5	75.8	77.1	0.756

**Table 5:** The testing results of AI'\_set.

Classifier	Accuracy (%)	Recall (%)	Precision (%)	F1 Score
Decision Tree	72.5	71.2	65.4	0.677
Random Forest	72.5	72.3	64.5	0.671
XGBoost	72.5	71.2	65.4	0.677

From Table 4, most models trained with  $AI'_{set}$  underperform that of the models trained with  $AI_{set}$  except the model trained with ANN classifier. By comparing the testing results, the models trained with  $AI_{set}$  (Table 3) outperforms the models trained with  $AI'_{set}$  (Table 5) for all classifiers. This suggests that the  $AI_{set}$  feature set is irreplaceable and confirms our earlier finding that the  $AI_{set}$  feature set is sufficient for our model development to classify foot arch types.

## 5 SYSTEM AND DESIGN

In this section, we describe the details of our system as the interface for interacting with our selected classification model, including system architecture, system structure chart, and some examples of user interfaces.

### 5.1 System Architecture

The system is implemented as a web application with three main components: a web application, web server, and classification module, as shown in Fig. 10. We use HTML, JavaScript, and Python for the web application. We implement a web server with a Python package called *Flask* [8]. Finally, the classification module is implemented using Python with the Scikit-learn package.

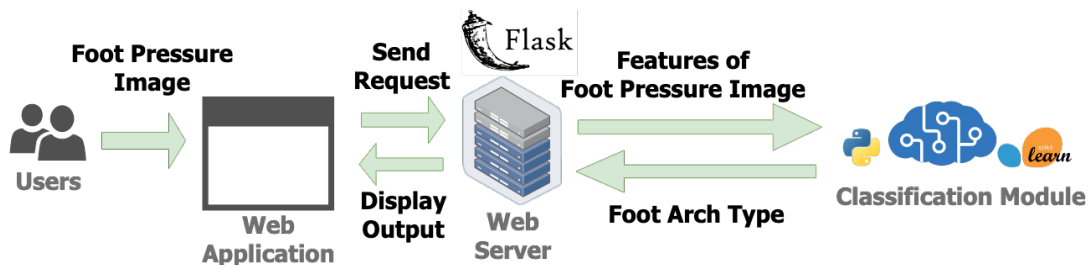


Figure 10: System Architecture.

Regarding this architecture, users submit an image or images to the web application. Then the web application sends a request to the web server. The web server performs pre-processing tasks. Next, the web server calls the classification module. Lastly, the classification module returns a foot arch type to users through the web server and web application.

### 5.2 System Structure Chart

*Foot Arch Type Classification System* (FAC) consists of two main modules as shown in Fig. 11. The first module is *User Interaction*. The second module is *Classification*.

1) *User Interaction*: This module provides functions for users to interact with the system, including

- Image Adding: Allow users to add foot pressure scanning images to be classified.
- Foot Arch Type Display: Display results of foot pressure scanning images.

2) *Classification*: This module performs the foot arch type classification task, including

- Image Getting: Obtain an image from the function Image Adding.
- Pre-processing: Apply the data pre-processing techniques in Section 2.1 such as Map-to-One.
- Feature Extraction: Extract all features in  $AI_{set}$  from the pre-processed image for classification.
- Classification Model: Apply the selected classification model on features to get a foot arch type.

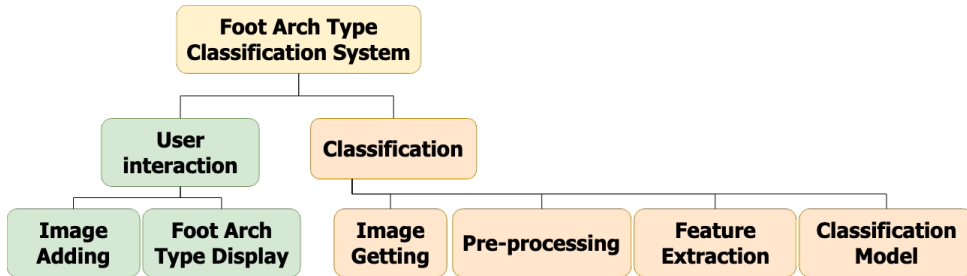


Figure 11: System Structure Chart.

### 5.3 User Interface

In this section, we present examples of our main user interface. Fig. 12 shows the user interface for uploading images. On this page, users upload an image or a set of images of foot pressure scanning for foot arch type classification. Fig. 13 shows the user interface for displaying foot arch type results to users.

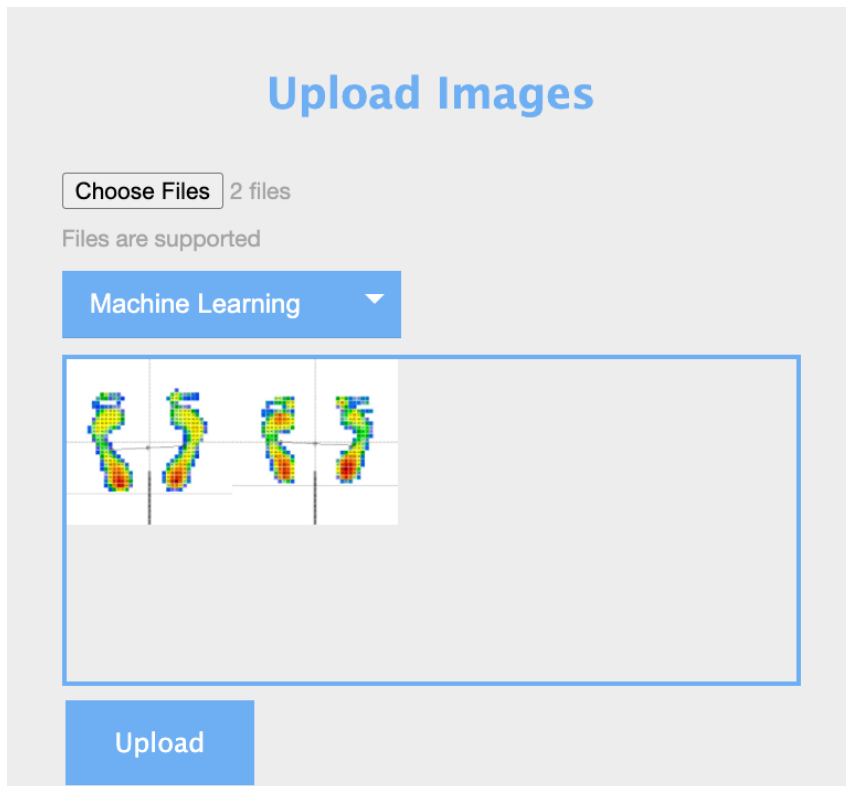


Figure 12: UI for uploading images.

File Name	Foot Type	
	Left	Right
1.jpg	Flat	Flat
4.jpg	Normal	Flat

**Figure 13:** UI for displaying foot arch type results.

## 6 CONCLUSIONS

In this research, supervised classification algorithms are used to develop models for classifying foot arch types from foot pressure scanning images. From the experimental results, the model trained with the decision tree classifier and AI\_set shows the best performance among the other classifiers in terms of accuracy, precision, recall, F1 score, and the number of features. In addition, the obtained decision tree model has a smaller number of hyperparameters than the other models. The results also demonstrate that the obtained model can classify foot arch types with high accuracy at 95%. Further, in this work, the FAC system has been implemented with the obtained classification model, which allows users to classify foot arch types from foot pressure scanning images easily.

To further improve the capability of classification of the system, more recent techniques such as convolutional neural networks (CNN) can be used. On the other hand, the new features of foot pressure scanning images can be extracted to improve the performance of classification as well.

## ACKNOWLEDGEMENT

We acknowledge the support from the Faculty of Information and Communication Technology, Mahidol University, Thailand. We would like to thank the National Metal and Materials Technology Center and, National Science and Technology Development Agency for their kind support on foot data for analysis.

While we are taking full responsibility for any remaining errors and shortcomings of the paper, we also thank the anonymous reviewers for their valuable input, that has greatly improved the quality of this paper.

## ORCID

Wudhichart Sawangphol, <http://orcid.org/0000-0001-7872-2482>

Pilailuck Panphattarasap, <http://orcid.org/0000-0003-0210-8237>

Pisit Praiwattana, <http://orcid.org/0000-0002-6710-7801>

Jidapa Krajangka, <http://orcid.org/0000-0002-4281-3603>

Thanapon Noraset, <http://orcid.org/0000-0002-7080-6523>

Danu Prommin, <http://orcid.org/0000-0002-8262-8293>

## REFERENCES

- [1] Breiman, L.: Random forests. *Machine learning*, 45(1), 5–32, 2001. ISSN 1573-0565. <http://doi.org/10.1023/a:1010933404324>.
- [2] Breiman, L.; Friedman, J.H.; Olshen, R.A.; Stone, C.J.: *Classification And Regression Trees*. Routledge, 2017. <http://doi.org/10.1201/9781315139470>.
- [3] Chen, T.; Guestrin, C.: Xgboost: A scalable tree boosting system. In *Proceedings of the 22nd acm sigkdd international conference on knowledge discovery and data mining*, 785–794, 2016. <http://doi.org/10.1145/2939672.2939785>.
- [4] Demšar, J.; Zupan, B.; Leban, G.; Curk, T.: Orange: From experimental machine learning to interactive data mining. In *Lecture Notes in Computer Science*, 537–539. Springer Berlin Heidelberg, 2004. [http://doi.org/10.1007/978-3-540-30116-5\\_58](http://doi.org/10.1007/978-3-540-30116-5_58).
- [5] Dufour, A.B.; Broe, K.E.; Nguyen, U.D.; Gagnon, D.R.; Hillstrom, H.J.; Walker, A.H.; Kivell, E.; Hannan, M.T.: Foot pain: is current or past footwear a factor? *Arthritis Care & Research*, 61(10), 1352–1358, 2009. ISSN 0004-3591. <http://doi.org/10.1002/art.24733>.
- [6] Fawcett, C.; Hoos, H.H.: Analysing differences between algorithm configurations through ablation. *Journal of Heuristics*, 22(4), 431–458, 2015. <http://doi.org/10.1007/s10732-014-9275-9>.
- [7] Glorot, X.; Bengio, Y.: Understanding the difficulty of training deep feedforward neural networks. In Y.W. Teh; D.M. Titterton, eds., *AISTATS*, vol. 9 of *JMLR Proceedings*, 249–256. JMLR.org, 2010. <http://dblp.uni-trier.de/db/journals/jmlr/jmlrp9.html#GlorotB10>.
- [8] Grinberg, M.: *Flask web development: developing web applications with python*. " O'Reilly Media, Inc.", 2018. ISBN 9781491991732.
- [9] Hawke, F.; Burns, J.: Understanding the nature and mechanism of foot pain. *Journal of Foot and Ankle Research*, 2(1), 2009. <http://doi.org/10.1186/1757-1146-2-1>.
- [10] Jian, M.S.; Shen, J.H.; Chen, Y.C.; Chang, C.C.; Fang, Y.C.; Chen, C.C.; Chen, W.H.: Study on cloud image processing and analysis based flatfoot classification approach. In *Current Topics on Mathematics and Computer Science Vol. 5*, 52–72. Book Publisher International (a part of SCIENCEDOMAIN International), 2021. <http://doi.org/10.9734/bpi/ctmcs/v5/3396f>.
- [11] Kotsiantis, S.B.; Zaharakis, I.D.; Pintelas, P.E.: Machine learning: a review of classification and combining techniques. *Artificial Intelligence Review*, 26(3), 159–190, 2006. <http://doi.org/10.1007/s10462-007-9052-3>.
- [12] Lee, H.J.; Lim, K.B.; Yoo, J.; Yoon, S.W.; Yun, H.J.; Jeong, T.H.: Effect of custom-molded foot orthoses on foot pain and balance in children with symptomatic flexible flat feet. *Annals of Rehabilitation Medicine*, 39(6), 905, 2015. <http://doi.org/10.5535/arm.2015.39.6.905>.
- [13] Luffy, L.; Grosel, J.; Thomas, R.; So, E.: Plantar fasciitis. *Journal of the American Academy of Physician Assistants*, 31(1), 20–24, 2018. <http://doi.org/10.1097/01.jaa.0000527695.76041.99>.
- [14] Menz, H.B.; Fotoohabadi, M.R.; Wee, E.; Spink, M.J.: Visual categorisation of the arch index: a simplified measure of foot posture in older people. *Journal of Foot and Ankle Research*, 5(1), 2012. <http://doi.org/10.1186/1757-1146-5-10>.
- [15] Montgomery, D.C.: *Design and analysis of experiments*. John Wiley & sons, 2017. ISBN 1119113474.
- [16] Pedregosa, F.; Varoquaux, G.; Gramfort, A.; Michel, V.; Thirion, B.; Grisel, O.; Blondel, M.; Prettenhofer, P.; Weiss, R.; Dubourg, V.; Vanderplas, J.; Passos, A.; Cournapeau, D.; Brucher, M.; Perrot, M.; Duchesnay, E.: Scikit-learn: Machine learning in Python. *Journal of Machine Learning Research*, 12, 2825–2830, 2011. <http://www.jmlr.org/papers/volume12/pedregosa11a/pedregosa11a.pdf>.
- [17] Queen, R.M.; Mall, N.A.; Hardaker, W.M.; Nunley, J.A.: Describing the medial longitudinal arch using

- footprint indices and a clinical grading system. *Foot & Ankle International*, 28(4), 456–462, 2007. <http://doi.org/10.3113/fai.2007.0456>.
- [18] Redmond, A.C.; Crosbie, J.; Ouvrier, R.A.: Development and validation of a novel rating system for scoring standing foot posture: The foot posture index. *Clinical Biomechanics*, 21(1), 89–98, 2006. <http://doi.org/10.1016/j.clinbiomech.2005.08.002>.
- [19] Roy, H.; Bhattacharya, K.; Deb, S.; Ray, K.: Arch index: an easier approach for arch height (a regression analysis). *Al Ameen Journal of Medical Sciences*, 5(2), 137–146, 2012.
- [20] Sawangphol, W.; Noraset, T.; Panphattarasap, P.; Praiwattana, P.; Sutthiratpanya, P.; Talanon, N.; Tungsupanich, K.; Prommin, D.: Foot arch posture classification using image processing. *Journal of Information Science and Technology*, 11(1), 75–82, 2021. ISSN 2651-1053. <http://doi.org/10.14456/JIST.2021.9>.
- [21] Sen, P.C.; Hajra, M.; Ghosh, M.: Supervised classification algorithms in machine learning: A survey and review, 99–111. Springer, 2020. [http://doi.org/10.1007/978-981-13-7403-6\\_11](http://doi.org/10.1007/978-981-13-7403-6_11).
- [22] Telfer, S.; Abbott, M.; Steultjens, M.; Rafferty, D.; Woodburn, J.: Dose–response effects of customised foot orthoses on lower limb muscle activity and plantar pressures in pronated foot type. *Gait & Posture*, 38(3), 443–449, 2013. <http://doi.org/10.1016/j.gaitpost.2013.01.012>.
- [23] Thai, L.H.; Hai, T.S.; Thuy, N.T.: Image classification using support vector machine and artificial neural network. *International Journal of Information Technology and Computer Science*, 4(5), 32–38, 2012. <http://doi.org/10.5815/ijitcs.2012.05.05>.
- [24] Thomas, M.J.; Roddy, E.; Zhang, W.; Menz, H.B.; Hannan, M.T.; Peat, G.M.: The population prevalence of foot and ankle pain in middle and old age: A systematic review. *Pain*, 152(12), 2870–2880, 2011. <http://doi.org/10.1016/j.pain.2011.09.019>.
- [25] Vařeka, I.; Vařeková, R.: The height of the longitudinal foot arch assessed by chippaux-Šmirák index in the compensated and uncompensated foot types according to root. *Acta Univ. Palacki. Olomuc*, 38(1), 35, 2008.
- [26] World, S.: Press cam v4.0, 2021. <https://www.sidasworld.co.uk/press-cam-v4-0/>.
- [27] Xiong, S.; Goonetilleke, R.S.; Witana, C.P.; Weerasinghe, T.W.; Au, E.Y.L.: Foot arch characterization: a review, a new metric, and a comparison. *Journal of the American Podiatric Medical Association*, 100(1), 14–24, 2010. ISSN 8750-7315. <http://doi.org/10.7547/1000014>.